Available online at www.sciencedirect.com
SCIENCE DIRECT
PERGAMON
Acta Astronautica 53 (2003) 779–787
ACTA ASTRONAUTICA
www.elsevier.com/locate/actaastro

MICROSCOPE IN ORBIT CALIBRATION PROCEDURE FOR A TEST OF THE EQUIVALENCE PRINCIPLE AT 10^{-15}

G.Pradels, P.Touboul
Physics and Instrumentation Department,
ONERA, Office National d'Etude et de Recherches Aérospatiales
F-92322 Châtillon CEDEX, France

Abstract: the scientific objectives of the MICROSCOPE space mission impose a very fine calibration of the on-board accelerometers. However the required performance cannot be achieved on ground because of the presence of high disturbing sources. On-board the CHAMP satellite, accelerometers similar in the concept to the MICROSCOPE instrument, have already flown and analysis of the provided data then allowed to characterise the vibration environment at low altitude as well as the fluctuation of the drag. The requirements of the in-orbit calibration procedure for the MICROSCOPE instrument are demonstrated by modelling the expected applied acceleration signals with the developed analytic model of the mission. The proposed approach exploits the drag-free system of the satellite and the sensitivity of the accelerometers. A specific simulator of the attitude control system of the satellite has been developed and tests of the proposed solution are performed using nominal conditions or disturbing conditions as observed during the CHAMP mission.

1. THE MICROSCOPE SPACE MISSION

1.1.Mission context

Since Galilee (1564-1642), the equivalence between the inertial and the gravitational mass has always been considered and in 1907 Einstein enounced the Equivalence Principle (EP) as the starting basement of his theory of General Relativity. Nevertheless the incompleteness of this theory is today pointed out, leading the modern physicists to seek for new interactions. But these new theories suppose EP violations at levels lower than 10^{-12} [1] which justifies the requirement of a very accurate EP test. To observe an eventual signal of EP violation, tests of the universality of free fall appear to be the most promising [2]. Experiments have already been performed like the Lunar laser ranging tests [3] which measures the acceleration ratio between the Earth and the Moon relatively to the Sun with a precision of 10^{-12}. Other recent tests, made in laboratory, concluded to accuracy of some 10^{-13} [4]. But the very quiet environment offered on board a satellite allows to improve the accuracy with a few order of magnitude. The goal of the MICROSCOPE space mission is the test the EP with an accuracy better than 10^{-15}.

1.2.Mission overview

MICROSCOPE (MICROSatellite pour l'Observation du Principe d'Equivalance) is a CNES fundamental physics space mission developed in co-operation with ESA. It will be the first one dedicated to perform the EP test in orbit with a satellite planed to be launched in 2006 for a one year mission duration. The sun-synchronous orbit is quasi polar at an altitude near 700km. The satellite weight will not exceed 150kg for a payload power less than 40W. The experiment is similar to a Galilee test with two test-masses made of different materials in a quasi-unlimited free fall around the Earth. The two masses are concentric to be submitted to the same gravity field and belong to the same instrument: a differential electrostatic accelerometer. The controlled electrostatic force necessary for maintaining them along the same orbit (with sub-nanometre accuracy) is measured along the Earth's pointing axis. According to the satellite (and so the instrument) pointing mode, the EP violation signal may appears at orbital frequency when the satellite is inertial pointing or at higher frequency when the satellite is rotating about the normal to the orbit axis. This later frequency is the sum (or the difference) of the orbital and rotation frequency.

1.3.Mission payload

The payload of the satellite is mainly composed of two differential accelerometers including each two electrostatic inertial sensors operating independently. Both differential accelerometers are identical except that one contains two test-masses of different material (Platinum and Titanium) while test-masses of the second are made in Platinum. The comparison between the measurements of the two differential accelerometers will help to reject

0094-5765/03/$ - see front matter © 2003 International Astronautical Federation. Published by Elsevier Science Ltd. All rights reserved
doi: 10.1016/S0094-5765(03)00114-0

systematic errors. For the selection of the material of the test-masses, a compromise between the theoretical interests and the required resolution for the instrument has been achieved by selecting the couple Platinum – Titanium [5].

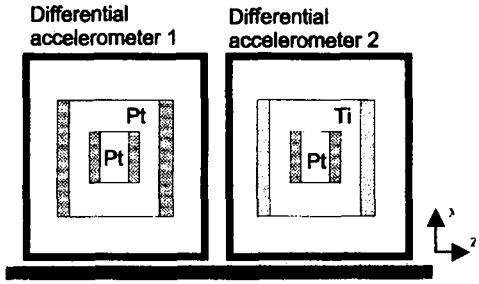

Figure 1: schema of the two differential accelerometers composed each of two cylindrical inertial sensors. The acceleration suffered by each test-mass is deduced from the knowledge of the necessary electrostatic forces to be applied by surrounding electrodes for maintaining the test-masses at their equilibrium position. An eventual violation of the EP is observed by comparing the acceleration suffered by the titanium and the platinum test-masses.

Along the cylinder axis (x-axis) motions of the test-masses are measured with a resolution of 6.10^{-10} m/√Hz and controlled with a resolution around 2.5 10^{-12} m/s²/√Hz [6]. Because the maximum measurement range of the inertial sensor is limited to 5.10^{-7} m/s² in High Resolution Mode, the satellite is equipped with a drag free and attitude control system (DFACS). This system uses the new technology of electrical thrusters FEEP (Field Emission Electric Propulsion) which equipped the satellite to apply continuously the thrusts that limit the level of the instrument linear acceleration to 3.10^{-10} m/s²/√Hz and of the angular acceleration to 10^{-8} rad/s²/√Hz. The control is performed by adequate servo-loop operating from the combination of the information delivered by all the onboard inertial sensors (accelerometer and star sensors).

1.4. Equations of motion

Let us note δ the EP violation term:

$$\delta=(m_g/m_i)_{masse1}-(m_g/m_i)_{masse2}.$$

Considering a reference frame centred at a point O, the acceleration measured by a single inertial sensor is:

$$\vec{\Gamma}_{meas}=\frac{\vec{F}_e}{m_i}\approx\frac{\vec{F}_{ng}}{M_i}+\left[\frac{M_g}{M_i}-\frac{m_g}{m_i}\right]\vec{g}(O)+([T]-[I])\overrightarrow{[G_1.G_{sat}]} \quad (1)$$

where F_e is the electrostatic force applied to the test-mass by the electrodes, F_{ng} the non-gravitational forces applied to the satellite, (m_i,Mi) and (m_g,M_g) the inertial and gravitational mass of respectively the test-mass and the satellite. g is the Earth's gravitational field, [T] and [I] the Earth's gravity gradient and the inertia tensors. G_1, G_{sat} the centre of mass of the test-mass and of the satellite.

For a differential accelerometer, the equation of the measurement is computed by the difference of each inertial sensor outputs. With (1), we obtain:

$$\vec{\Gamma}_{measured,diff}=\delta.\vec{g}(o)+([T]-[I])\overrightarrow{G_1G_2} \quad (2)$$

To reach an accuracy of 10^{-15}, the second term of the last equation has to be reduced either by limiting the distance between the two masses or the amplitude of the Earth's gravity gradient acting at the same frequency as the EP signal. This requires to estimate the test-mass off-centering and the expression of the Earth's gravity gradient in the instrumental frame.

The mean value of both inertial sensor outputs provides an estimation of the common acceleration necessary to the DFACS to counteract the satellite surface forces:

$$\vec{\Gamma}_{measured,com}=\overrightarrow{\Gamma_{ng}}+([T]-[I])\left(\overrightarrow{G_1G_{sat}}+\overrightarrow{G_2G_{sat}}\right) \quad (3)$$

Precedent experiments in space, like the CHAMP mission, offered the possibility to study some of these perturbations occurring on a small satellite at low altitude. In preparation of the MICROSCOPE mission, analysis of these data has been performed.

2. THE CHAMP SPACE MISSION

2.1. Mission overview

The CHAMP mission is a geodesic space mission from the German space agency in collaboration with CNES and JPL to recover the Earth's gravity field [7]. The satellite is equipped with different instruments and in particular the STAR accelerometer and a GPS receiver. The satellite obits at an altitude of 460 km in a quasi-polar orbit along an Earth's pointing mode.

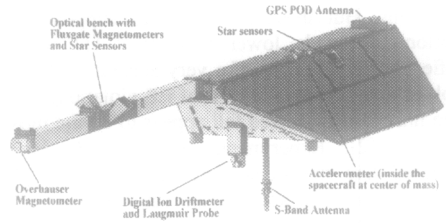

Figure 2 : the CHAMP satellite with the different on-board instruments. The accelerometer STAR measures the non-gravitational forces applied to the satellite.

The STAR accelerometer [8] is a three axis electrostatic accelerometer, similar to the

MICROSCOPE mission instrument but includes a parallelepiped test-mass. Situated close to the centre of mass of the satellite, less than 5 mm, the instrument measures the non-gravitational forces with a resolution of 10^{-9} m/s²/√Hz.

2.2. Observation of the in-orbit disturbances

Figure 3 shows the measurements provided by the STAR accelerometer on October 2000, the 21. These data are not filtered but corrected from an identified problem by a post-treatment detailed in [9]. The radial X-axis corresponds at low frequency to a very quiet signal, sum of the instrument bias, the terrestrial infrared, pressure and the Earth's albedo. The Y-axis, along the track, is mainly representative to the atmospheric density variations characterised by fluctuations at the orbital frequency of about 5.10^{-7}ms^{-2}. The Z-axis, normal to the orbit plane, is also sensitive to the atmospheric drag linked to the Earth's rotation or to the winds. Nevertheless, all of these geodesic signatures have been disturbed by high frequency and non-stationary signals.

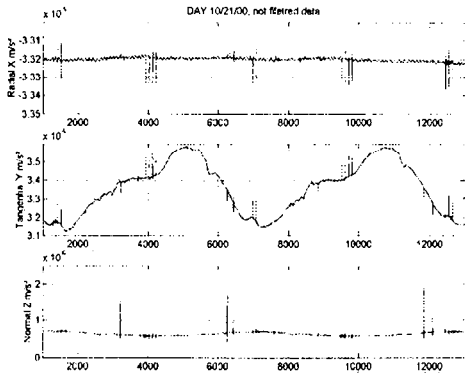

Figure 3 : measurements provided by the STAR accelerometer on-board the CHAMP satellite on the October 2000, the 21.

Let us note the following identified disturbances:

- Peaks of low amplitude (few 10^{-8} m/s²) are often observed on the 3 linear axes (figure 5). Tests at the ONERA laboratory demonstrated the correlation with the heaters switch on/off in conjunction with behaviour of the accelerometer sole pate made of aluminium.
- Quickly damped (few seconds) oscillations are observed on the X and Z axis. They are due to the satellite arm (figure 6) carrying the magnetometer and which mechanical mode is excited by the thruster actuation.
- Peaks of high amplitude can be observed after the satellite crossing of the Earth's shadow because of the high thermal gradient suffered by the structure of the satellite.

The figure 5 and 6 with expanded time scale illustrate these perturbations.

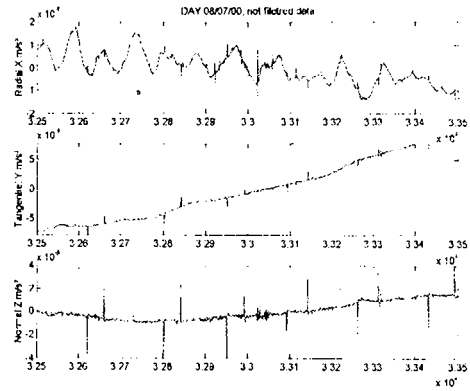

Figure 4: measured peaks of a few 10^{-8} m/s² correlated to the inner thermal active control of the satellite. (The DC part has been here canceled).

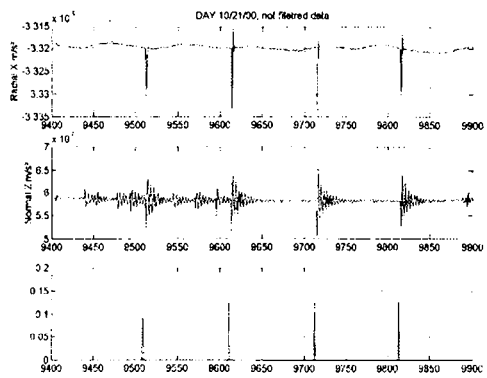

Figure 5: oscillations due to the satellite arm after thruster firings. The third graph represents the duration of the thrust.

2.3. Temporal analysis

In order to clean the geodesic signal from some disturbances, a specific filter has been developed [10]. After filtering, the bias of the linear axis and the thermal sensitivity are assessed by a temporal analysis. It concludes to the good performances of the STAR accelerometer in regards to the expected values estimated on ground during the development phase of the instrument [8].

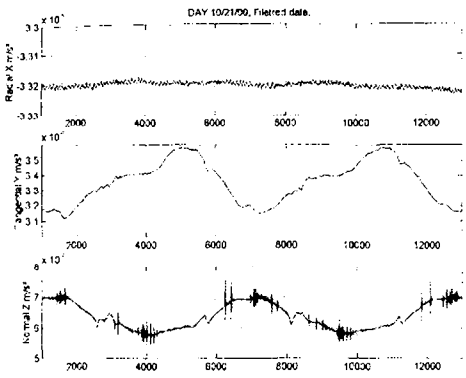

Figure 6 : filtered signals of previous figure 4. The X-axis output is quite constant with a quasi stationary signal of weak amplitude $10^{-8}ms^{-2}$ at $5.10^{-2}Hz$, signal which could be due to the satellite attitude control. The Y-axis is cleaned of the high frequency peaks. On the expanded Z-axis, the peaks (a few seconds duration) have been suppressed while oscillations of much lower amplitude are still observed to be analysed.

Tab 1compares the mean value of the in-orbit measurement to the overvaluation of the instrument bias estimated from production specifications. Tab 2 provides estimates of the bias thermal sensitivity with respect to the temperature measured on board the satellite close to the test-mass.

Bias estimation/ Axis	From data m/s^2	On ground m/s^2
X	$-64.41\ 10^{-6}$	$1.21\ 10^{-4}$
Y	$33.55\ 10^{-7}$	$1.6\ 10^{-5}$
Z	$6.24\ 10^{-7}$	$1.6\ 10^{-5}$

Tab 1 : comparison between the bias of the instrument assessed by the measurements in space and the theoritical values estimated on ground before the launch.

Thermal sensitivity estimation	From data $m/s^2/°C$	On-ground $m/s^2/°C$
X	$4\ 10^{-8}$	$2.73\ 10^{-8}$
Y-Z	$<2\ 10^{-7}$	$5.75\ 10^{-9}$

Tab 2 : bias thermal sensitivities, evaluated in orbit and during instrument development. Y and Z sensitivities are difficult to be evaluated in orbit because of the weak temperature fluctuations and sensitivities.

The subtraction of the filtered measurements (Figure 6) from the not filtered one (Figure 3) provides an estimation of the measured in-orbit disturbances. In the next chapter these data are used to test the proposed calibration procedure for the MICROSCOPE mission.

2.4. Frequency analysis

From the performed spectrums of the measurements (figure 8), an overvaluation of the accelerometer intrinsic noise level has been assessed and compared to the instrument specifications (Tab 3). This overvaluation is the spectrum level at higher frequencies where the vibration environment is softer.

High frequency level estimation	From data $m/s^2/\sqrt{Hz}$	Specifications over 1 Hz $m/s^2/\sqrt{Hz}$
X	$3\ 10^{-9}$	10^{-8}
Y	$8\ 10^{-10}$	2.10^{-9}
Z	$3\ 10^{-9}$	2.10^{-9}

Tab 3 : comparison of the high frequency level measured on the data provided by CHAMP and the level estimated on-ground before launch.

On the Z-axis spectrum, lines just before 3.10^{-1} Hz are clearly observed but the correspondence with the temporal representation of the signal (figure 6) help to conclude that the lines correspond to a superposition of non-stationary oscillations and are produced by the satellite structural behaviour excited by the thermal environment and the thruster activation

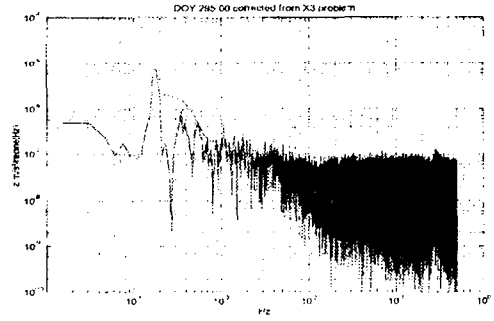

Figure 7: spectrum of the Z-axis output. The blue curve corresponds to the spectral density of the non-filtered signal with great peaks, the green to the filtered signal and the red to a mean of 4 successive spectrums. The line at 3.10^{-1} Hz is the superposition of different oscillations of the satellite arm measured by the accelerometer.

2.5. Time-Frequency analysis

A time frequency analysis using the Short Fourier or the Wigner-Ville transforms is performed to characterise the lines observed on spectrums of the X and Z axis. The figure 9 shows the time evolution of the vibration spectrum which helps to confirm the nature of the lines at about 310^{-1} Hz and that the oscillations observed on the Z-axis are of same frequency.

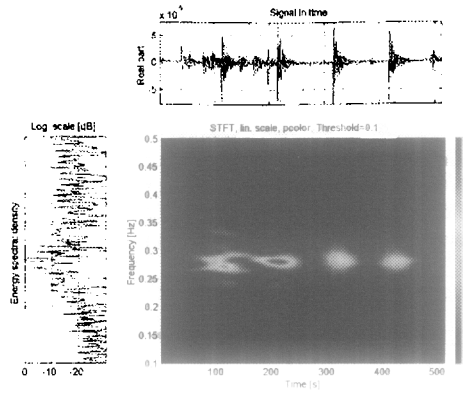

Figure 8: time-frequency analysis of the Z-axis measurement. At several 10^{-1}Hz, non-stationary oscillations are observed and correspond to the satellite structural behaviour.

Another representation is considered by performing mean over one day of the spectrums and by juxtaposing these spectrums along one month as shown on figure 10. This representation is used to detect the specific days with unusual behaviours or very soft conditions. In addition, this representation allows to observe the amplitude evolution of the low frequency lines corresponding for instance to the drag (figure 10): measured along the Y-axis, the drag depends on the orientation of the orbit with respect to the sun.

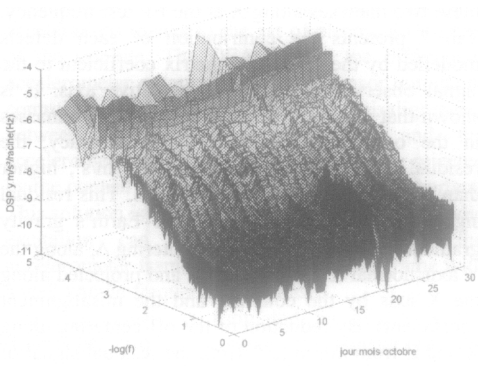

Figure 9: mean spectrums of the Y-axis over one month. This tools has been developed to identify unusual behaviours as here the day 17. But it could be used to observe the evolution of the amplitude of the low frequencies.

2.6.Synthesis

In addition to the precise measurements of the non-gravitational external forces applied on the satellite, the CHAMP mission offered for the first time the possibility to analyse other and non expected in-orbit disturbances. The analysis of the data is also the opportunity to test the concept and the performances of the inertial sensor in orbit and to confirm the maturity of this technology.

For the MICROSCOPE mission a peculiar care is taken to limit these disturbances. For instance, a sun-synchronous orbit with no shadow crossing is selected, the satellite is compact and stiff and the inner thermal control is passive... The developed techniques to suppress the disturbing peak signals and to detect and analyse the non stationary ones are useful for the MICROSCOPE data processing (the EP signal being stationary and quite sine wave shape).

3. PROCEDURE OF CALIBRATION FOR THE MICROSCOPE INSTRUMENT

Considering the scientific objectives of the MICROSCOPE space mission and the precedent perturbations, a fine calibration procedure is necessary to value the amplitude of the instrument sensitivity matrixes and to correct the scientific measurements by a posterior data treatment. Neither the test-masses nor the electrodes of the instrument are indeed perfectly cylindrical, positioned and aligned (2μm tolerance on the part geometry). These defects might generate sin wave or random signals higher than the required limit of a few 10^{-15} m/s². On ground, a dedicated test bench decoupled from seismic vibrations has been developed in our laboratory to verify the performances of the accelerometers. The residual level of external perturbations (few 10^{-9} m/s²/√Hz) prohibits any calibration of the instrument with the accuracy required by the space experiment. Free fall tests can also be performed at the specific Drop Tower in Bremen (Germany) [11] but the fall duration (4.7 seconds) and the vibrating environment delivered by the falling capsule (a few 10^{-7}m/s²/√Hz) are not compatible with the necessary estimate of the instrument sensitivity. Then, an in-orbit calibration procedure must be developed.

3.1. Model of the instrument

The following analytical model of the output of the three axis inertial sensor is considered:

$$\Gamma_{meas} = K_0 + M_1 \Gamma_{app} + \Gamma_{noise} \quad (4)$$

where K_0 is a column vector (3x1) representing the instrument bias along the 3 instrument sensitive axes, M_1 a (3x3) matrix representing the sensitivity matrix of the inertial sensor and Γ_n a column vector of the intrinsic noise. The diagonal of the M matrix represents the instrument scale factor. The non-

diagonal terms of the matrix are equal to the sum of the instrument couplings between the measurements axes and the misalignments angles with the reference frame. The star sensor frame is for the experiment the reference frame because the provided data and models will be expressed with respect to his frame. From equation (4), the differential accelerometer measurement, $\Gamma_{meas,diff}$, is expressed by introducing the differential mode (half the difference) and the common mode (half the sum) of the two measurements delivered by each inertial sensor. This decomposition leads to the following equation with M_{com} and M_{diff} being two matrixes representing respectively the common and the differential mode of the differential accelerometer sensitivity:

$$\begin{pmatrix}\Gamma_{meas,com}\\ \Gamma_{meas,diff}\end{pmatrix}=\begin{pmatrix}K_{0,com}\\ K_{0,diff}\end{pmatrix}+M\begin{pmatrix}\Gamma_{app,com}\\ \Gamma_{app,diff}\end{pmatrix}+\begin{pmatrix}\Gamma_{noise,com}\\ \Gamma_{noise,diff}\end{pmatrix}$$

$$\text{where}\quad M=\begin{pmatrix}M_{com} & M_{diff}\\ M_{diff} & M_{com}\end{pmatrix} \qquad (5)$$

The real differential acceleration applied to the instrument is then deduced by inverting (5):

$$\Gamma_{app,diff}=\begin{pmatrix}A_{diff} & A_{com}\end{pmatrix}\left[\begin{pmatrix}\Gamma_{meas,com}\\ \Gamma_{meas,diff}\end{pmatrix}-\begin{pmatrix}\Gamma_{noise,com}\\ \Gamma_{noise,diff}\end{pmatrix}-\begin{pmatrix}K_{0,com}\\ K_{0,diff}\end{pmatrix}\right]$$

$$\text{with}\ A_{diff}=M_{diff}^{-1}\ \text{and}\ A_{com}=M_{com}^{-1} \qquad (6)$$

The equation (6) shows that the A_{diff} matrix introduces the common mode of the measured acceleration (residual drag...) while A_{com} introduces the differential mode of the measured acceleration (gravity gradient, attitude motions... depending on the distance between the two masses). The in-orbit calibration of the instrument consists thus in the estimation of these two matrixes in order to obtain the true acceleration Γ_{app} from the measurement acceleration Γ_{meas}. Before describing the calibration method, the objectives for the performance of the instrument calibration must be defined in accordance with the EP test accuracy.

3.2. In-orbit calibration performances

The fine in-orbit calibration of the differential accelerometer is only required for the most sensible axis (X axis) along which the EP signal is observed. To establish the calibration objectives, a typical MICROSCOPE orbit has been finely computed with a mean eccentricity of 10^{-2}, a 720 km altitude and an inclination of 98.4° [12]. From these data and from the expected performances of the DFACS (Tab 4), the acceleration amplitudes measured by a perfect differential accelerometer (A_{com} = I, A_{diff} = 0) are computed for two values of the distance between the two test-masses (see Tab 5). In all the following analysis, the satellite is inertial pointing; same approach can be conducted with rotating satellite. In Tab 5, harmonic of the signal at orbital frequency is provided because this is the frequency observed for the detection of the eventual violation signal. With a perfect instrument, the measured signal in differential mode along the X sensitive axis is 1.5 10^{-15} m/s² much less than 10^{-15} times the gravity field of 7.9 m/s² at 700 km altitude. In the same manner, the 2 10^{-13} m/s²/√Hz is compatible with the 10^{-15} accuracy taking into account the selected 10^5 seconds integration period of the provided data.

	Frequency (Hz)	X-Y-Z	Unit
Angular velocity	DC	10^{-6}	rad/s
	Noise	10^{-6}	rad/s/√Hz
Angular acceleration	DC	2 10^{-6}	rad/s²
	1.710^{-4} - 210^{-3}	10^{-8}	rad/s²/√Hz
	210^{-3} – 10^{-2}	10^{-7}	rad/s²/√Hz
Linear acceleration	DC (*)	10^{-9}	m/s²
	1.710^{-4} - 210^{-3}	3 10^{-10}	m/s²/√Hz
	210^{-3} – 10^{-2}	3 10^{-9}	m/s²/√Hz

Tab 4: requirements on the performances of the drag free system (DFACS) used to reduce the amplitude of the non-gravitational accelerations suffered by the satellite. (*) : when the DFACS is not disturbed by the accelerometer bias level.

A total level of 10^{-15} m/s² has been specified for the disturbing level introduced after data filtering at the EP frequency by the matrixes A_{diff} and A_{com} for actual instrument. Values deduced from machining tolerances (Tab 6) are used to estimate the disturbing amplitudes introduced by each term of these two matrixes along X at the EP test frequency. Tab 7 presents the contribution of each defects modelled by the sensitivity matrix coefficient to the signal observed along the X sensitive axis. It is shown that even with a centering of the two masses in the orbit plane with a 0.1μm accuracy, the residual measured signal is 1.9 10^{-14} m/s², higher than the 10^{-15} m/s² specification level. This residual signal is in fact the effect of the Earth's gravity gradient introduced by the off-centering Δ, along the Y axis normal to the orbit plane and projected along the X axis by the coupling and the misalignment coefficients. By reduction of the off-centering along X and Z from 20μm to 0.1μm, the residual signal of 1.9 10^{-13} m/s² has not been divided in the same ratio. The required accuracy for the A_{com} matrix elements (major contributors as shown in Tab 7) depends thus on the amplitude of Δ and is expressed by $\Delta.A_{com} <$ 7.5 10^{-9} rad.m. Considering the amplitude of the residual common applied acceleration, the A_{diff} matrix must be estimated with a 1.5 10^{-4} rad accuracy. These two values are related to the 10^{-15} m/s² specified residual level and in particular to the orbit eccentricity of 10^{-2}.

Measured signal by perfect instrument Δx,y,z = 20μm	Common mode signal X	Common mode signal YZ	Differential mode signal X	Differential mode signal Y	Differential mode signal Z	Unit
At orbital frequency, harmonic	10^{-12}	10^{-12}	$1.8\ 10^{-13}$	$6.9\ 10^{-13}$	$5.0\ 10^{-13}$	m/s²
Near orbital frequency, √PSD	$3\ 10^{-10}$	$3\ 10^{-10}$	$4\ 10^{-13}$	$3\ 10^{-13}$	$5\ 10^{-13}$	m/s²/√Hz
Δx,z =0.1μm Δy =20 μm						
At orbital frequency, harmonic	10^{-12}	10^{-12}	$1.5\ 10^{-15}$	$6.9\ 10^{-13}$	$2\ 10^{-15}$	m/s²
Near orbital frequency, √PSD	$3\ 10^{-10}$	$3\ 10^{-10}$	$2\ 10^{-13}$	$2\ 10^{-14}$	$2\ 10^{-13}$	m/s²/√Hz

Tab 5 : with the support of (2) and (3), the signals measured by a perfect differential accelerometer is computed for the common and differential mode considering two values of the distance between the two test-masse along the X and Z axis. The PSD is power spectral density of the signal

Term	A_{diff}	A_{com}
Diagonal	$+/- 10^{-2}$	$1+/- 10^{-2}$
Non-diagonal	$+/- 10^{-3}$	$+/- 10^{-2}$

Tab 6 : non-calibrated values of the instrument defects deduced from the machining tolerances.

Defects matrixes	Difference of the applied signal Δx,y,z=20μm	Difference of the applied signal Δx,z=0.1μm
$A_{com}(1,1)$ - 1	1.8E-15	1.5E-17
$A_{com}(1,2)+ A_{com}(1,3)$	3.3E-15	6.8E-15
$A_{diff}(1,1)$	1.0E-14	1.0E-14
$A_{diff}(1,2)+ A_{diff}(1,3)$	2.0E-15	2.0E-15
Sum	1.7E-14	1.8E-14
Applied difference	1.8E-13	1.5E-15
Measured difference	1.9E-13	1.9E-14

Tab 7 : the instrument measurement along the X-axis is computed taking into account the matrix of sensibility before calibration.

3.3.In-orbit calibration procedure

But the difficulty comes from the lack of identified acceleration signal in the accelerometer frame. The proposed procedure consists in applying successive accelerations thanks to the set of electrical thrusters of the satellite. The DFACS uses the differential accelerometer outputs and the star sensor outputs to control the satellite motion. The misalignments between the frame of the FEEP and the accelerometer or the star sensor frames are rejected by the control loop gains and thus not too important. This solution is very interesting because the periodic excitation can be either performed in the accelerometer frame or in the star sensor frame with a well known frequency and phase.

The A_{diff} matrix is estimated by observing the differential mode measurements considering the common mode when 3 periodic translations along the accelerometer axes are performed. The amplitude and the frequency of the excitation signal can be selected inside the inertial sensor range and bandwidth. A 5.10^{-3} Hz frequency limits the amplitude of the systematic error due to the higher harmonics of the gravity gradient and situates the calibration signal sufficiently close to the frequency of the test. An excitation amplitude of 10^{-8} m/s² and an integration period of the measured signal extended to 1/2 orbit (~3000s) are compatible with the required $1.5\ 10^{-4}$ accuracy for estimate the A_{diff} matrix.

The A_{com} matrix is more difficult to estimate. It requires indeed to create 3 periodic signals of differential mode (rotation of the satellite) in order to create inertial forces of high amplitude in the linear differential measurement. By this way a linear system of 3 equations can be resolved to estimate the required elements of the A_{diff} matrix. However, it requires the excitation to be performed at low frequency lower than few 10^{-3} Hz, inside the star sensor frequency bandwidth. Considering the amplitude of the statistic error, due to the intrinsic noise of the accelerometer, and the sum of the systematic errors, due to the instrument couplings and the residual angular velocity at DC, a frequency of 10^{-3}Hz, an integration period of 4 orbits and an oscillation angle of 0.6 rad at least are required to estimate the A_{com} matrix elements with the required accuracy of $7.5\ 10^{-4}$ rad when Δ<10μm.

The angular calibrated motions of the satellite are also useful for the estimation of the test-mass off-centering (Δ). Differential acceleration proportional to Δ are generated and measured at the rotation frequency (angular acceleration) or higher frequency (centrifugal acceleration).

Δ can also be calibrated by exploiting the differential signal induced by the Earth's gravity gradient at twice the orbital frequency (inertial pointing satellite) but contrarily to the precedent method, the off-centering along the normal to the orbit axis (Y axis) cannot be recovered.

The presented calibration procedure does not require any supplementary system onboard the satellite. Only the existing sensors, actuators and all the data provided from the instruments themselves are exploited.

3.4.Calibration procedure tests

A software simulator (Figure 10) for the test of the proposed calibration procedures has been developed with the MatLab/Simulink software. The model of

the differential accelerometer includes the sensitivity matrix of each inertial sensor and their detailed transfer function. The overall transfer function of the DFACS is also implemented including the hybridization between the star sensor and the accelerometer measurement. The FEEP misalignments and gains are also considered. The precalculated data of the Earth's gravity field and gradient used in paragraph 3.2 are introduced to produce the accelerations suffered by the satellite. The elements to be calibrated (sensitive matrixes and test-masses off-centering) are randomly drawn in accordance to values of Tab 6.

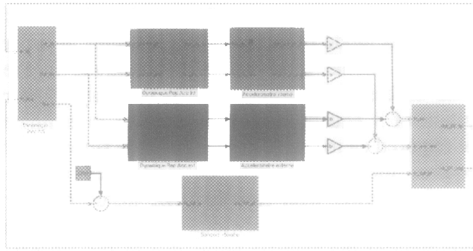

Figure 10: snapshot of the Simulink model of the DFACS loop. Both transfer function of the inertial sensors and of the DFACS are simulated. The instrument defects as the bias, the intrinsic noise, the misalignments and the couplings are inserted. This simulator allows to check the validity of the proposed calibration method for different type of orbital mode or environment and will be used to analyse the in flight data.

The Figure 11 is the Fourier transform of the differential mode measurement along the X axis with a time window of 3000 seconds (1/2 orbit) when a common mode excitation of 10^{-8} m/s² at 5 10^{-3}Hz along X is performed during the calibration phase. The amplitude of the line at 5 10^{-3} Hz allows the estimation of the first element of the A_{diff} matrix.

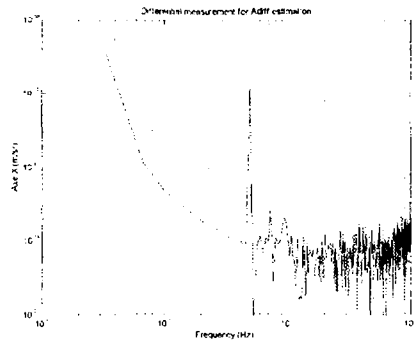

Figure 11: Fourier transform of the differential measurement of the ultra-sensitive axis X computed by the simulator. These data have been obtained after 3000 seconds of integration with a sampling frequency of 8 Hz. At low frequency, we observe the Earth's gravity gradient components and at 5.10^{-3}Hz the peak due to the linear excitation introduced by the difference of the inertial sensor sensitivity. At upper frequencies the residual non-gravitational accelerations out of the DFACS bandwidth is observable.

Figure 12 is also a Fourier transform of the differential mode measurement along X but for a time window of 24000 seconds (4 orbits) and when an excitation of differential mode is performed at 10^{-3} Hz. The amplitude of the measured acceleration at 10^{-3} Hz is the product of the inertial acceleration applied in the (Y-Z) accelerometer frame due to the satellite rotation with the common misalignments A_{com} between the star sensor and the differential accelerometer.

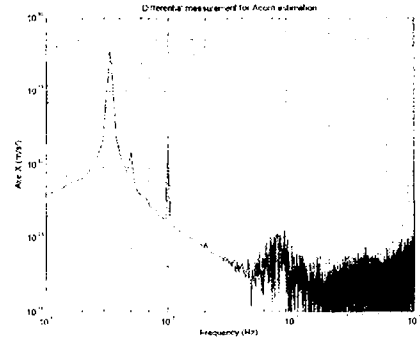

Figure 12: Fourier transform of the differential measurement of the axis X computed with 240000 seconds of integration with a sampling frequency of 8 Hz. At low frequency, we observe the Earth's gravity gradient components at twice the orbital frequency (inertial satellite pointing) and at 1.10^{-3}Hz the peak due to the differential excitation introduced by the rotation of the satellite and the test-mass off-centering. At 2 10^{-3} Hz, the small line is due to the centrifugal acceleration.

All the cases of excitations have been simulated and table 14 provides the obtained calibration accuracy for the X axis and in the case of a 10^{-2} eccentricity of the inertial orbit.

	Initial value	Estimated value	Absolute difference	Required accuracy
$A_{com}(1,2)$	-2.68 10^{-3}	-2.80 10^{-3}	1.3 10^{-4}	6.3 10^{-4}
$A_{com}(1,3)$	2.32 10^{-3}	2.40 10^{-3}	0.8 10^{-4}	4.3 10^{-4}
$A_{diff}(1,1)$	-1.44 10^{-3}	-1.43 10^{-3}	0.1 10^{-4}	1.5 10^{-4}
$A_{diff}(1,2)$	0.05 10^{-3}	0.06 10^{-3}	0.1 10^{-4}	1.5 10^{-4}
$A_{diff}(1,3)$	-0.04 10^{-3}	-0.03 10^{-3}	0.1 10^{-4}	1.5 10^{-4}
Δ_x (µm)	12.33	12.26	0.07	0.1
Δ_y	11.85	11.80	0.06	0.1
Δ_z	*17.53*	*17.60*	*0.07*	*0.1*

Tab 14: comparison between the matrix coefficient input values and estimations related to the X axis. The required accuracyfor the MICROSCOPE mission is indicated in the last column.

The in-orbit perturbations added to the expected gravitational or drag signals and observed on the

CHAMP measurement along the six axes of the instrument are now used to test the calibration procedure in a disturbed environment. Figure 13 shows, the addition of the disturbing signals deduced from the CHAMP data with the precalculated non-gravitational accelerations acting on the MICROSCOPE satellite. First tests are performed with the simulator and conclude to the possibility of the instrument calibration with the required accuracy. Further investigation are undertaken to assess the robustness of the calibrated procedure to the satellite vibrating environment.

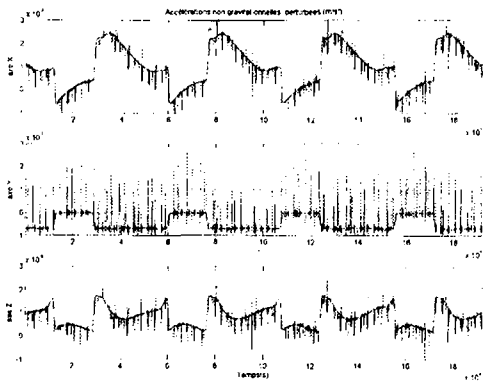

Figure 13: superposition of the precalculated non-gravitational acceleration acting on the MICROSCOPE satellite and the disturbing signals observed on the CHAMP mission measurements.

4. CONCLUSION

The MICROSCOPE space mission aims at the test of the Equivalence Principle with a minimum accuracy of 10^{-15}. Besides the outstanding resolution of the inertial sensors, the experiment demands a very fine calibration of the three axes of the instrument sensitivities. The specification of this calibration is clearly related to the residual acceleration environment onboard the drag free satellite at the 700 km altitude.

With the CHAMP mission, the STAR accelerometer measures finely the non-gravitational forces applied on the satellite at low altitude between 500km and 400km. The return of this mission was of most importance for the development of future projects by the analysis of disturbances occurring on board such a satellite.

The MICROSCOPE drag free system allows to perform the necessary in-orbit calibration of the instrument in orbit without stringent added constraints on the propulsion system. Taking into account the acceleration environment, the procedures of the calibration of both inertial sensors have been proposed and the obtained accuracy is in agreement with the 10^{-15} EP.

The developed software simulator is used to optimise the possibility of the instrument calibration according to the performance of each subsystem, propulsion, drag-free loop, instrument.This simulator prepares also the analysis of the data that will be collected after the satellite launch foreseen in 2006.

5. REFERENCES

[1]T.Damour, *Violations of the equivalence principle in a dilaton-runaway scenario.* IHES/P/02/27,Bicocca FT-02-03, CERN-TH/2002-093

[2]T.Damour, *Questioning the equivalence principle*, C.R.Acad.Sci.Paris, 2001, t.2,p1249.

[3]Dickey J.O. et al, Science 256 (1994) 482.

[4]Baessler S. et al, *Imroved Test of the Equivalence Principle for the Gravitational Self-Enegy*, Physical Review Letters, 1999, vol13, n°18

[5]Blaser J.P, *Tests-mass material selection for STEP*, 1996, Clas. & Quant.Gravity, vol 13, n°11A

[6]M.Rodrigues, *MICROSCOPE Payload Documentation Phase A,* RT/606063 ONERA, May 2002.

[7] Ch.Reigber et al. 'CHAMP mission statut', Adv. Space Res. Vol30 N°2 p129-134,2002

[8]P. Touboul, B. Foulon *Accelerometer STAR. Definition Report.* (issue 1).-RT 10/3805 DMPH/Y

[9]B.Foulon et al., *Accéléromètre STAR : Analyse du comportement de l'électrode X3*, janvier 2002, ONERA RT

[10]G.Pradels, *Traitement des données CHAMP*, 2000, ONERA RT

[11]H.Dittus, A new experimental baseline for testing the weak equivalence principle at the Bremen drop tower, Class. Quantum Grav. 18 (2001) 2417-2425.

[12]Gille Metris, *Simulations et analyses pour la mission MICROSCOPE*, personale note, 2002